Paratunamides A−D, Oxindole Alkaloids from *Cinnamodendron axillare*

Toshinori Kagata,[†] Shizuka Saito,[†] Hideyuki Shigemori,[§] Ayumi Ohsaki,[‡] Haruaki Ishiyama,[†] Takaaki Kubota,[†] and Jun'ichi Kobayashi*[,†]

Graduate School of Pharmaceutical Sciences, Hokkaido University, Sapporo 060-0812, Japan, Institute of Applied Biochemistry, University of Tsukuba, Tsukuba, Ibaraki, 305-8572, Japan, and Institute of Biomaterials and Bioengineering, Tokyo Medical and Dental University, Tokyo 101-0062, Japan

Received June 25, 2006

Four new oxindole alkaloids, paratunamides A−D (**1**−**4**), containing a secologanin unit, were isolated from the bark of *Cinnamodendron axillare*, and their structures and relative configurations were elucidated by spectroscopic data. The absolute configuration at C-7 in **1**−**4** was assigned as *S*, *S*, *R*, and *S*, respectively, on the basis of the CD spectra.

In our search for structurally unique compounds from Brazilian medicinal plants,[1−8] four new oxindole alkaloids, paratunamides A−D (**1**−**4**), containing a secologanin unit, were isolated from *Cinnamodendron axillare* (Nees at Mart.) (family Canellaceae) (local name paratude). In Brazil "paratude" is used as a stomachic and a treatment for tonsillitis. In this paper, we describe the isolation and structure elucidation of **1**−**4**.

The MeOH extract of the bark of *C. axillare* was partitioned between EtOAc and H_2O, and then the aqueous layer was extracted with *n*-BuOH. The *n*-BuOH-soluble portions were subjected to silica gel column chromatography ($CHCl_3$/MeOH, 6:1) and then a C_{18} reversed-phase column (MeOH/H_2O (33:67) → MeOH) to afford an alkaloidal fraction, which was purified by C_{18} HPLC (CH_3CN/H_2O, 20:80) to yield paratunamides A (**1**, 0.0021%), B (**2**, 0.0041%), C (**3**, 0.0026%), and D (**4**, 0.00077%). The EtOAc-soluble portions were separated on a silica gel column ($CHCl_3$/MeOH, 95:5) to give the two known alkaloids strictosamide (**5**)[9] and pumiloside (**6**).[10]

The molecular formula $C_{27}H_{34}N_2O_{11}$ of paratunamide A (**1**) was established by HRFABMS [*m/z* 585.2052 $(M + Na)^+$, Δ −0.8 mmu]. The IR spectrum implied the presence of hydroxy (3409 cm^{-1}), lactam (1712 cm^{-1}), and α,β-unsaturated carbonyl (1648 cm^{-1}) groups. The gross structure of **1** was deduced from detailed analysis of ^1H and ^{13}C NMR data (Table 1) aided with 2D NMR experiments ($^1H-^1H$ COSY, HMQC, and HMBC). The ^{13}C NMR data indicated that the molecule possessed two lactam carbonyls, six aromatic carbons, one trisubstituted olefin (one carbon of which was attached to an ether oxygen), one monosubstituted olefin, two hemiacetal carbons, one aminal carbon, one oxygenated sp^3 quaternary carbon, four oxymethines, one oxymethylene, one methoxy, three methylenes (one of which was bearing an nitrogen atom), and two methines. The $^1H-^1H$ COSY spectrum revealed connectivities of C-5 to C-6, C-9 to C-12, C-3 to C-14, C-14 to C-15, C-18 to C-21, C-15 to C-20, and C-1′ to C-6′ (Figure 1). HMBC correlations of H-9 to C-7 (δ_C 77.19) and C-13 (δ_C 143.40), H-12 to C-8 (δ_C 133.51), and H_2-6 to C-2 (δ_C 182.33) and C-7 revealed the presence of an oxindole ring, in which a hydroxy group was attached to C-7 (Figure 1). The presence of a δ-lactam ring, which was fused to a dihydropyran ring, was elucidated by HMBC correlations of H-3 to C-22 (δ_C 166.98), H-15 and H-21 to C-16 (δ_C 109.50), and H-17 to C-15 (δ_C 24.00), C-21 (δ_C 98.60), and C-22. The connectivity between the oxindole ring and the δ-lactam ring through an ethylene unit (C-5 and C-6) was elucidated by HMBC correlations of H_2-6 to C-2 and C-7, H_2-5 to C-22, and H-3 to C-5. The $^1H-^1H$ coupling constants ($J_{1',2'}$ = 7.8 Hz) and the ^{13}C NMR data of the anomeric carbon (δ_C 100.82), oxymethines (δ_C 72.3, 75.45, 78.76, and 79.10), and oxymethylene (δ_C 63.47) indicated the presence of a β-D-glucopyranosyl moiety. HMBC correlations of MeO-3 (δ_H 3.39, s) to C-3, H-21 to C-1′, and H-1′ to C-21 (δ_C 98.60) indicated that the methoxy group and the glucose were attached at C-3 and C-21, respectively. Thus, the structure of paratunamide A was elucidated to be **1**.

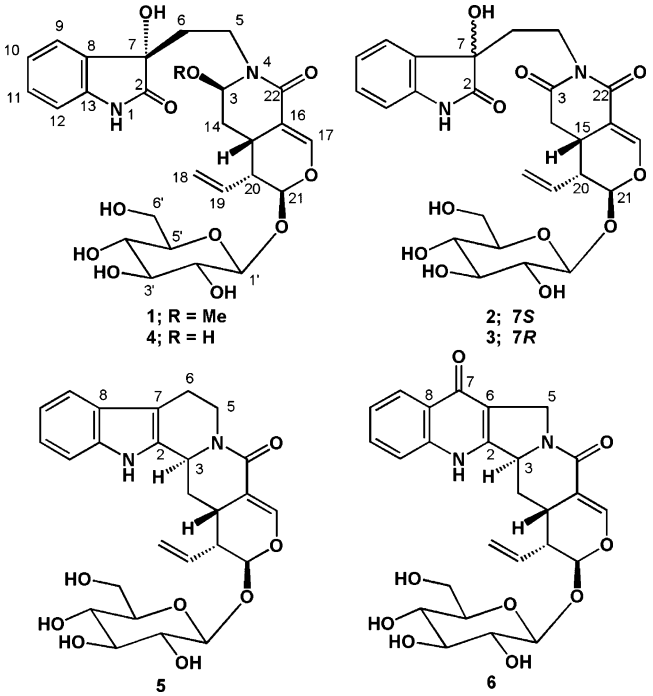

NOESY correlations of H-14a to H-3 and H-15, H-20 to H-15 and H-21, and H-14b to H-3 and H-19 and $^1H-^1H$ coupling constants indicated a half-chair conformation of the δ-lactam ring, α-orientations of H-3 and H-21, and β-orientations of H-15 and H-20 (Figure 2). Therefore, the relative configuration of paratunamide A was assigned as **1**. The absolute configuration at C-7 of **1** was elucidated to be *S*, since the CD spectra of **1** exhibited a negative Cotton effect in the 260−300 nm wavelength region and a positive Cotton effect in the 220−260 nm wavelength region (Figure 5).[11]

Paratunamide B (**2**) showed the pseudomolecular ion peak at *m/z* 547 $(M + H)^+$ in the FABMS. HRFABMS analysis revealed the molecular formula to be $C_{26}H_{30}N_2O_{11}$ [*m/z* 547.1906 $(M + H)^+$, Δ −2.2 mmu]. The ^1H and ^{13}C NMR spectra of **2** were similar to those of paratunamide A (**1**) except for the δ-lactam moiety. The

* Corresponding author. Tel: +81-11-706-3239. Fax: +81-11-706-4989. E-mail: jkobay@pharm.hokudai.ac.jp.
[†] Hokkaido University.
[§] University of Tsukuba.
[‡] Tokyo Medical and Dental University.

10.1021/np0602968 CCC: $33.50
Published on Web 09/30/2006

Table 1. ^{1}H and ^{13}C NMR Data of Paratunamide A (**1**) in CD_3OD

position	^{1}H[a]		*J* (Hz)	^{13}C[a]	HMBC	NOESY
1	10.26[b]					
2				182.33	H-6a, 6b	
3	4.71	dd	3.4, 2.6	90.15	MeO-3	H-5a, 5b, 6a, 14a, 14b, MeO-3
4						
5 (a)	3.64	m		43.84	H-3, 6a, 6b	H-3, 6a, 6b
5 (b)	3.25	m				H-3, 6a, 6b
6 (a)	2.24	dd	6.0, 2.6	37.72		H-3, 5a, 5b, 9
6 (b)	2.23	dd	6.0, 2.6			H-5a, 5b
7				77.19	H-6a, 6b	
8				133.51	H-10, 12	
9	7.40	d	7.4	125.94	H-11	H-6a
10	7.10	dd	7.8, 7.4	124.62	H-9, 12	
11	7.30	dd	7.8, 7.4	131.46	H-9	
12	6.92	d	7.4	112.11	H-10	
13				143.40	H-9, 11	
14 (a)	2.01	ddd	13.8, 3.4, 3.4	29.34		H-3, 15, MeO-3
14 (b)	1.50	ddd	14.1, 13.8, 2.6			H-3, 19
15	3.24	m		24.00	H-3, 17, 21	H-14a, 20
16				109.50	H-17, 20	
17	7.37	d	2.6	150.11	H-21	
18 (a)	5.32	dd	17.5, 1.9	121.17		H-19, 20
18 (b)	5.29	dd	10.1, 1.9			H-19, 20
19	5.55	ddd	17.1, 10.1, 10.1	134.96	H-14b, 18a, 18b	
20	2.61	ddd	10.1, 6.0, 1.8	44.86	H-17	H-15, 18a, 18b, 21
21	5.49	d	1.8	98.60	H-17, 1′	H-20, 1′
22				166.98	H-3, 5a, 5b, 17	
3-OMe	3.39	s		57.14		H-3, 14a
1′	4.68	d	7.8	100.82	H-21, 2′	H-21
2′	3.21	m		75.45	H-3′	
3′	3.38	m		78.76	H-2′, 4′	
4′	3.31	m		72.30	H-6′	
5′	3.34	m		79.10	H-4′	
6′ (a)	3.92	dd	11.9, 1.9	63.47		
6′ (b)	3.69	dd		11.9, 6.0		

[a] In ppm. [b]Observed in DMSO-d_6.

^{1}H−^{1}H COSY spectrum revealed connectivities of C-5 to C-6, C-9 to C-12, C-14 to C-15, C-18 to C-21, C-15 to C-20, and C-1′ to C-6′ (Figure 3). HMBC correlations of H-9 to C-7 (δ_C 77.23) and C-13 (δ_C 143.85), H-12 to C-8 (δ_C 131.48), and H_2-6 to C-2 (δ_C 182.16) and C-7 revealed the presence of an oxindole ring, in which a hydroxy group was attached to C-7 (Figure 3). The presence of a dihydropyran ring, which was connected to a β-D-glucopyranosyl moiety at C-21 (δ_C 98.55), was elucidated by HMBC correlations of H-17 to C-15, C-16 (δ_C 108.62), and C-21. HMBC correlations of H_2-5 to C-3 (δ_C 174.53) and C-22 (δ_C 167.94), H_2-14 to C-3, and H-17 to C-22 revealed the presence of a glutarimide moiety (C-3, C-14−C-16, C-22, and N-4), which was fused to the dihydropyran ring. The relative configuration of paratunamide B was assigned as **2** on the basis of NOESY correlations and ^{1}H−^{1}H coupling constants (Figure 4). The absolute configuration at C-7 was elucidated to be *S*, since a negative Cotton effect in the 260−300 nm wavelength region and a positive Cotton effect in the 200−260 nm wavelength region were observed in the CD spectrum of **2** (Figure 5).

The molecular formula $C_{26}H_{30}N_2O_{11}$ of paratunamide C (**3**) indicated by HRFABMS [*m/z* 547.1949 $(M + H)^+$, Δ +2.1 mmu] was the same as that of **2**. The ^{1}H and ^{13}C NMR spectra were very similar to those of **2**. The gross structure of **3** was the same as that of **2** on the basis of ^{1}H−^{1}H COSY and HMBC correlations of **3**. The relative configuration of paratunamide C was assigned as **3** by ^{1}H−^{1}H coupling constants and NOESY correlations. Compound **3** showed the nearly antipodal CD spectrum of **2** (Figure 5), suggesting that **3** was the epimer at C-7 of **2**.

Paratunamide D (**4**) showed the pseudomolecular ion peak at *m/z* 571 $(M + Na)^+$ in the FABMS. HRFABMS analysis revealed

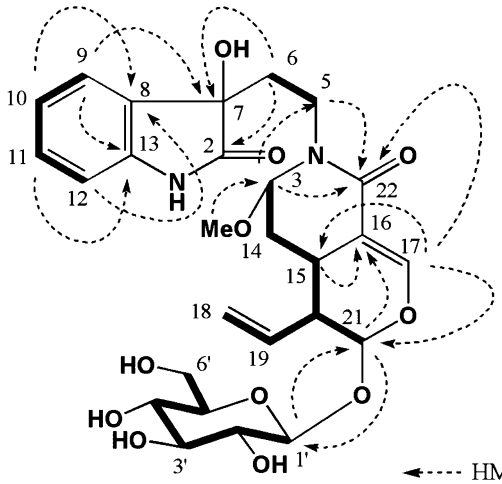

Figure 1. ^{1}H−^{1}H COSY and selected HMBC correlations of paratunamide A (**1**).

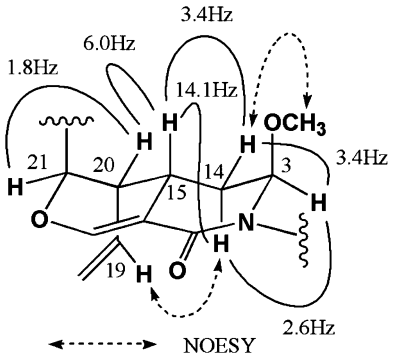

Figure 2. Relative configuration of δ-lactam and dihydropyran rings of paratunamide A (**1**).

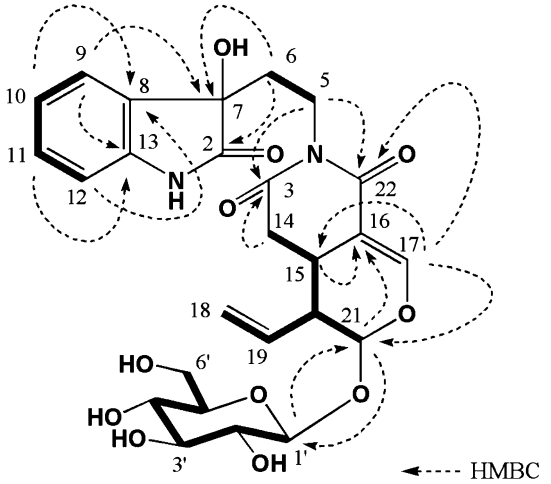

Figure 3. ^{1}H−^{1}H COSY and selected HMBC correlations of paratunamide B (**2**).

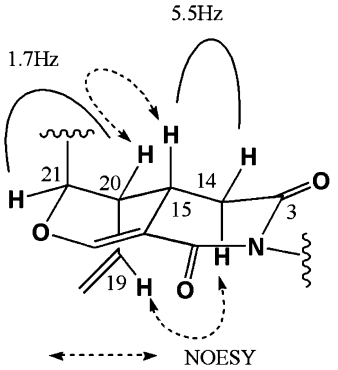

Figure 4. Relative configuration of δ-lactam and dihydropyran rings of paratunamide B (**2**).

the molecular formula to be $C_{26}H_{32}N_2O_{11}$ [*m/z* 571.1874 $(M + Na)^+$, Δ −3.0 mmu]. The ^{1}H and ^{13}C NMR spectra of **4** were similar to those of paratunamide A (**1**) except for signals (δ_H 3.39; δ_C 57.14) for the methoxy group at C-3 in **1**, which were absent in **4**. In addition, the difference between ^{1}H and ^{13}C NMR chemical shifts for positions 3 and 14 of **1** and those of **4** also indicated that **4** was the *O*-demethyl form of **1**. The ^{1}H−^{1}H COSY spectrum revealed connectivities of C-5 to C-6, C-9 to C-12, C-3 to C-14, C-14 to C-15, C-18 to C-21, C-15 to C-20, and C-1′ to C-6′. The gross structure of paratunamide D was elucidated by HMBC correlations. The relative configuration of **4** was derived from NOESY correlations and ^{1}H−^{1}H coupling constants. The absolute configuration at C-7 was elucidated to be *S* on the basis of the CD spectra of **4** (Figure 5).

Paratunamides A−D (**1**−**4**) are new oxindole alkaloids containing a secologanin unit from *C. axillare* (Nees at Mart.). This type of monoterpene oxindole alkaloids is very rare, although a 7-hydroxyoxindole alkaloid has been obtained from the leaves of *Uncaria salaccensis*.[12] Biogenetically, paratunamides A−D (**1**−**4**) may be derived from strictosamide (**5**) through oxidative cleavage between the C-2 and C-3 bond (Scheme 1),[13] while it has been proposed that pumiloside (**6**) is biosynthesized by the autoxidation−recyclization at C-2, C-6, and C-7 from **5**.[14] On standing in MeOH for several days exposed to air, strictosamide (**5**) was slowly converted into pumiloside (**6**), which suggests that pumiloside (**6**) could be an autoxidation product of strictosamide (**5**).

Paratunamide D (**4**) showed moderate cytotoxicity against human epidermoid carcinoma KB cells (IC_{50} = 6 μg/mL) in vitro, while paratunamides A−C (**1**−**3**) did not show such activity (IC_{50} > 10 μg/mL).

Experimental Section

General Experimental Procedures. Optical rotations were recorded on a JASCO DIP-370 polarimater. CD, IR, and UV spectra were recorded on JASCO J-720, JASCO FT/IR-230, and JASCO Ubest-35 spectrophotometers, respectively. ^{1}H and ^{13}C NMR spectra were recorded on a Bruker AMX-600 spectrometer using 2.5 mm micro cells (Shigemi Co., Ltd). The 3.35 and 49.8 ppm resonances of residual MeOH-d_4 were used as internal references for ^{1}H and ^{13}C NMR spectra, respectively. FAB mass spectra were obtained using glycerol as a matrix.

Plant Material. The bark of *C. axillare* was purchased from Farmaervas in São Paulo, Brazil. The plant was identified by Dr. G. Hashimoto (Centro de Pesquisas de História Natural, São Paulo, Brasil),

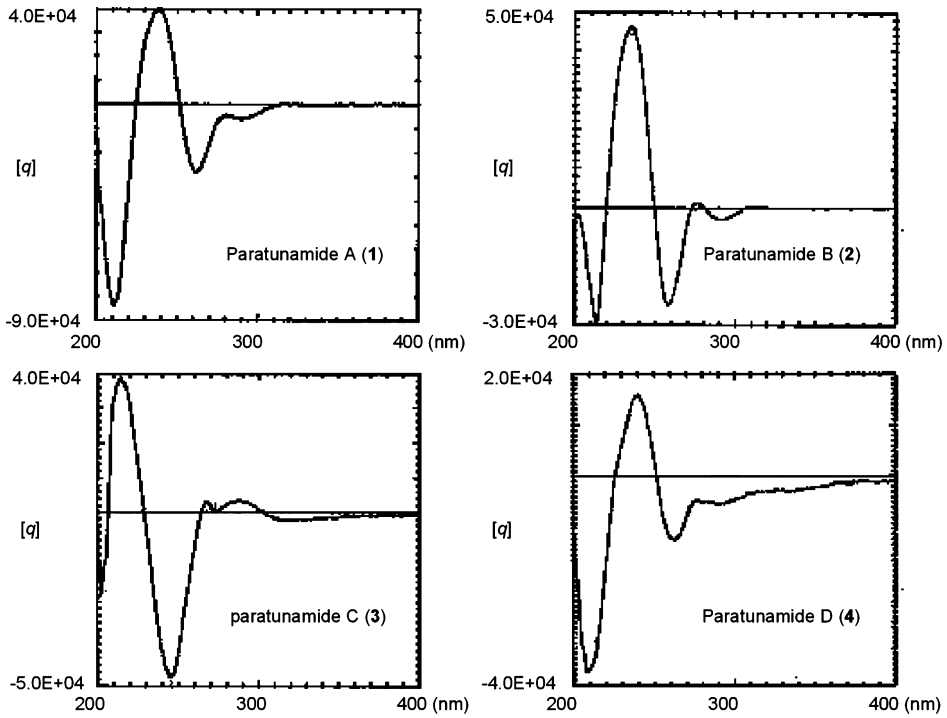

Figure 5. CD spectra of paratunamides A−D (**1**−**4**) in MeOH.

Scheme 1. Plausible Mechanism of Formation of Paratunamides A−D (**1**−**4**) and Pumiloside (**6**) from Strictosamide (**5**)

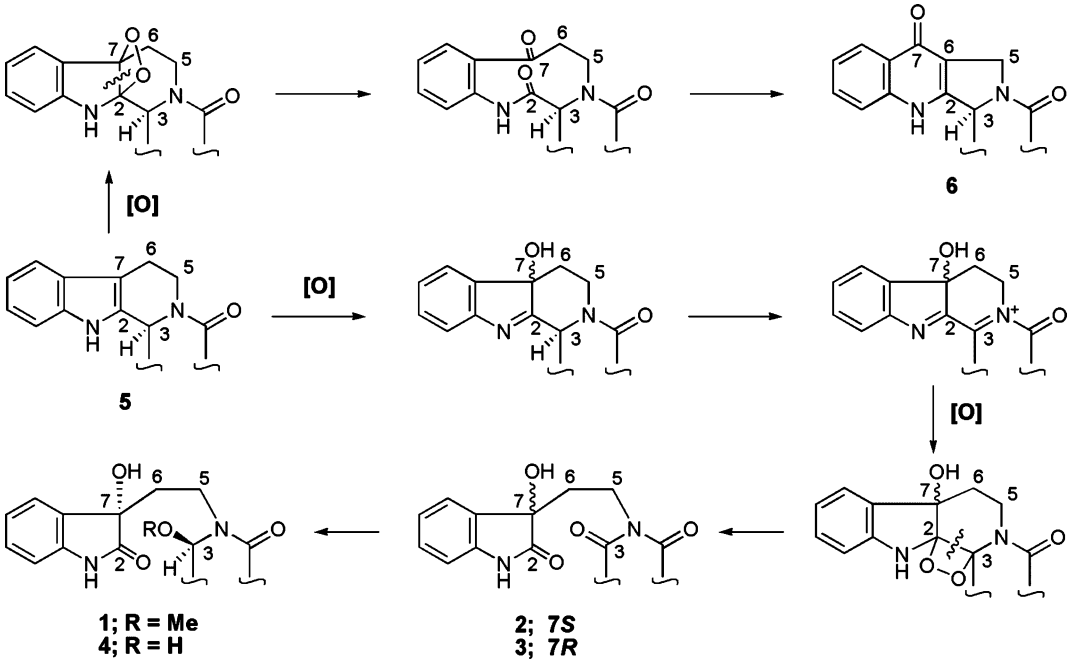

Table 2. ^{1}H and ^{13}C NMR Data of Paratunamides B (**2**), C (**3**), and D (**4**) in CD_3OD

	2		**3**		**4**	
position	$^{1}H^{a}$	$^{13}C^{a}$	$^{1}H^{a}$	$^{13}C^{a}$	$^{1}H^{a}$	$^{13}C^{a}$
1	10.18 (s)[b]		10.23 (s)[b]		10.23 (s)[b]	
2		182.16		182.20		
3		174.53		174.41	5.01 (dd, 3.0,3.0)	80.82
4						
5 (a)	3.85 (m)	36.92	3.85 (m)	36.87	3.68 (m)	42.70
5 (b)	3.69 (m)		3.76 (m)		3.24 (m)	
6 (a)	2.27 (m)	36.69	2.27 (t, 6.9)	36.63	2.28 (m)	37.47
6 (b)	2.26 (m)		2.27 (t, 6.9)		2.18 (m)	
7		77.23		77.23		77.20
8		131.48		131.55		133.50
9	7.36 (d, 7.2)	125.94	7.39 (d, 7.2)	126.00	7.41 (d, 7.8)	125.42
10	7.10 (dd, 7.8,7.2)	124.57	7.10 (dd, 7.6,7.2)	124.53	7.11 (t, 7.8)	124.02
11	7.29 (dd, 7.8,7.7)	133.03	7.30 (dd, 7.9,7.8)	133.14	7.29 (t, 7.8)	131.07
12	6.91 (d, 7.7)	112.27	6.91 (d, 7.9)	112.22	6.92 (d, 7.8)	111.52
13		143.85		143.77		143.40
14 (a)	2.46 (dd, 15.1,5.5)	35.62	2.46 (dd, 16.2,5.6)	35.53	1.78 (m)	33.81
14 (b)	2.35 (dd, 15.1,14.1)		2.28 (dd, 16.2,14.2)		1.60 (td, 14.1,3.0)	
15	3.21 (m)	25.22	3.21 (m)	25.25	3.34 (m)	23.78
16		108.62		108.66		109.50
17	7.54 (d, 2.2)	153.29	7.59 (d, 2.3)	153.29	7.36 (d, 2.6)	149.12
18 (a)	5.32 (dd, 16.8,1.9)	122.51	5.36 (dd, 15.2,1.5)	122.59	5.32 (dd, 17.1,1.9)	120.44
18 (b)	5.29 (dd, 10.0,1.9)		5.35 (dd, 12.0,1.5)		5.27 (dd, 10.5,1.9)	
19	5.55 (m)	133.98	5.60 (m)	134.01	5.55 (dt, 17.1,10.5)	134.11
20	2.71 (m)	44.69	2.70 (m)	44.75	2.60 (m)	44.78
21	5.61 (d, 1.7)	98.55	5.61 (d, 1.3)	98.62	5.51 (d, 1.9)	97.75
22		167.94		168.15		166.98
1′	4.72 (d, 8.0)	100.37	4.70 (d, 8.1)	100.53	4.70 (d, 8.2)	100.05
2′	3.21 (m)	75.56	3.21 (m)	75.46	3.22 (m)	75.25
3′	3.38 (m)	78.79	3.38 (m)	78.58	3.41 (m)	78.40
4′	3.31 (m)	72.35	3.31 (m)	72.32	3.32 (m)	72.07
5′	3.34 (m)	79.22	3.35 (m)	79.19	3.34 (m)	78.55
6′ (a)	3.92 (dd, 12.0,2.0)	63.50	3.92 (m)	63.49	3.92 (m)	63.05
6′ (b)	3.68 (m)		3.68 (m)		3.70 (m)	

[a] In ppm. [b]Observed in DMSO-d_6.

and a voucher specimen has been deposited at Institute of Biomaterials and Bioengineering, Tokyo Medical and Dental University.

Extraction and Separation. The bark (50 g) was extracted with MeOH (500 mL × 3), and the extracts were partitioned between EtOAc (50 mL × 3) and H_2O (50 mL). Then the aqueous layer was extracted with *n*-BuOH. The *n*-BuOH-soluble portions were subjected to silica gel column chromatography ($CHCl_3$/MeOH, 6:1), a C_{18} column (MeOH/H_2O, 25:75), and then C_{18} reversed-phase HPLC (Capcell Pak RP-18, Shiseido Co. Ltd, 1.0 × 25 cm; flow rate 2.5 mL/min; UV detection at 254 nm; eluent CH_3CN/H_2O, 20:80) to afford paratunamides A (**1**, 0.8 mg), B (**2**, 1.6 mg), C (**3**, 1.0 mg), and D (**4**, 0.3 mg). The EtOAc-soluble portions were separated by a silica gel column ($CHCl_3$/MeOH, 95:5) to give strictosamide (**5**, 10 mg) and pumiloside (**6**, 15 mg).

Paratunamide A (1): colorless, amorphous solid; $[\alpha]^{24}_{D}$ −98.5 (*c* 0.15, MeOH); UV (MeOH) λ_{max} 209 (ϵ 23 600) and 239 (14 700) nm; IR (KBr) ν_{max} 3409, 1712, 1648, and 1628 cm^{-1}; CD (MeOH) 211

($\Delta\epsilon$ −25.4), 238 (+12.1), 262 (−8.5), 280 (−1.4), and 290 (−1.9) nm; ^{1}H and ^{13}C NMR (Table 1); FABMS *m/z* 585 $(M + Na)^+$; HRFABMS *m/z* 585.2052 $(M + Na)^+$ (calcd for $C_{27}H_{34}N_2O_{11}Na$, 585.2060).

Paratunamide B (2): colorless, amorphous solid; $[\alpha]^{24}_D$ −71.4 (*c* 0.73, MeOH); UV (MeOH) λ_{max} 212 (ϵ 22 800) and 249 (12 200) nm; IR (KBr) ν_{max} 3429, 1715, 1659, and 1621 cm^{-1}; CD (MeOH) 214 ($\Delta\epsilon$ −9.0), 235 (+14.0), 258 (−7.5), 278 (+0.4), and 291 (−0.9) nm; ^{1}H and ^{13}C NMR (Table 2); FABMS *m/z* 547 $(M + H)^+$; HRFABMS *m/z* 547.1906 $(M + H)^+$ (calcd for $C_{26}H_{30}N_2O_{11}$, 547.1928).

Paratunamide C (3): colorless, amorphous solid; $[\alpha]^{24}_D$ −63.8 (*c* 0.77, MeOH); UV (MeOH) λ_{max} 208 (ϵ 37 600) and 246 (14 700) nm; IR (KBr) ν_{max} 3427, 1714, 1660, and 1621 cm^{-1}; CD (MeOH) 214 ($\Delta\epsilon$ +11.8), 246 (−14.3), 267 (+0.9), 273 (+0.1), and 287 (+1.0) nm; ^{1}H and ^{13}C NMR (Table 2); FABMS *m/z* 547 $(M + H)^+$; HRFABMS *m/z* 547.1949 $(M + H)^+$ (calcd for $C_{26}H_{30}N_2O_{11}$, 547.1928).

Paratunamide D (4): colorless, amorphous solid; $[\alpha]^{24}_D$ −24.9 (*c* 0.43, MeOH); UV (MeOH) λ_{max} 205 (ϵ 30 700) and 232 (13 600) nm; IR (KBr) ν_{max} 3417, 1712, 1655, and 1623 cm^{-1}; CD (MeOH) 209 ($\Delta\epsilon$ −11.3), 240 (+4.8), 263 (−3.6), 275 (−1.4), and 292 (0) nm; ^{1}H and ^{13}C NMR (Table 2); FABMS *m/z* 571 $(M + Na)^+$; HRFABMS *m/z* 571.1874 $(M + Na)^+$ (calcd for $C_{26}H_{32}N_2O_{11}Na$, 571.1904).

Acknowledgment. We thank Dr. G. Hashimoto (Centro de Pesquisas de História Natural, São Paulo, Brazil) for identification of *C. axillare*, and Ms. S. Oka and Ms. M. Kiuchi (Center for Instrumental Analysis, Hokkaido University) for measurements of FABMS. This work was partly supported by a Grant-in-Aid for Scientific Research from the Ministry of Education, Science, Sports and Culture of Japan.

References and Notes

(1) Kobayashi, J.; Sekiguchi, M.; Shigemori, H.; Ohsaki, A. *J. Nat. Prod.* **2000**, *63*, 375−377.
(2) Kobayashi, J.; Sekiguchi, M.; Shigemori, H.; Ohsaki, A. *Tetrahedron Lett.* **2000**, *41*, 2939−2943.
(3) Sekiguchi, M.; Shigemori, H.; Ohsaki, A.; Kobayashi, J. *J. Nat. Prod.* **2001**, *64*, 1102−1106.
(4) Shigemori, H.; Shimamoto, S.; Sekiguchi, M.; Ohsaki, A.; Kobayashi, J. *J. Nat. Prod.* **2002**, *65*, 82−84.
(5) Sekiguchi, M.; Shigemori, H.; Ohsaki, A.; Kobayashi, J. *J. Nat Prod.* **2002**, *65*, 375−376.
(6) Kobayashi, J.; Sekiguchi, M.; Shimamoto, S.; Shigemori, H.; Ishiyama, H.; Ohsaki, A. *J. Org. Chem.* **2002**, *67*, 6449−6455.
(7) Takashima, J.; Komiyama, K.; Ishiyama, H.; Kobayashi, J.; Ohsaki, A. *Planta Med.* **2005**, *71*, 1−5.
(8) Ishiyama, H.; Matsumoto, M.; Sekiguchi, M.; Shigemori, H.; Ohsaki, A.; Kobayashi, J. *Heterocycles* **2005**, *66*, 651−658.
(9) Aimi, N.; Shito, T.; Fukushima, K.; Itai, Y.; Aoyama, C.; Kunisawa, K.; Sakai, S.-I.; Haginiwa, J.; Yamasaki, K. *Chem. Pharm. Bull.* **1982**, *30*, 4046−4051.
(10) Aimi, N.; Nishimura, M.; Miwa, A.; Hoshino, H.; Sakai, S.-I.; Haginiwa, J. *Tetrahedron Lett.* **1989**, *30*, 4991−4994.
(11) The absolute configuration at C-7 of 7-hydroxyoxindole alkaloids has been elucidated by comparison of the CD spectra with those of known 7-hydroxyoxindole compounds of which the absolute configuration has been established. Takayama, H.; Shimizu, T.; Sada, H.; Harada, Y.; Kitajima, M.; Aimi, N. *Tetrahedron* **1999**, *55*, 6841−6846. Labroo, R. B.; Cohen, L. A. *J. Org. Chem.* **1990**, *55*, 4901−4904.
(12) Ponglux, D.; Wongseripipatana, S.; Aimi, N.; Nishimura, M.; Ishikawa, M.; Sada, H.; Haginiwa, J.; Sakai, S. *Chem. Pharm. Bull.* **1990**, *38*, 573−575.
(13) Shigemori, H.; Kagata, T.; Kobayashi J. *Heterocycles* **2003**, *59*, 275−281.
(14) Carte, B. K.; DeBrosse, C.; Eggleston, D.; Hemling, M.; Mentzer, M.; Poehland, B.; Troupe, N.; Westley, W.; Hecht, S. M. *Tetrahedron* **1990**, *46*, 2747−2760.

NP0602968